Eur. Cytokine Netw. Vol. 33, n° 1, *March 2022* 13-24

RESEARCH ARTICLE

IL-27 attenuates airway inflammation and epithelial-mesenchymal transition in allergic asthmatic mice possibly via the RhoA/ROCK signalling pathway

Chuanjun Huang[1,2], Yan Sun[2], Na Liu[2], Ziping Zhang[1], Xiyan Wang[2], Degan Lu[2], Ling Zhou[2,a], Caiqing Zhang[3,a]

[1] Department of Respiratory Diseases, Shandong University of Traditional Chinese Medicine, Jinan, Shandong 250013
[2] Department of Respiratory Medicine and critical care, The First Affiliated Hospital of Shandong First Medical University & Shandong Provincial Qianfoshan Hospital, Jinan, Shandong 250014
[3] Department of Respiratory Diseases, Department of Otolaryngology-Head and Neck Surgery, Shandong Provincial ENT Hospital, Cheeloo College of Medicine, Shandong University, Jinan, Shandong 250014

Correspondence: Professor Caiqing Zhang, Department of Otolaryngology-Head and Neck Surgery, Shandong Provincial ENT Hospital, Cheeloo College of Medicine, Shandong University. Duanxingxi Road, Huaiyin, Jinan, Shandong 250000, P.R. China
Professor Ling Zhou, department of Respiratory Medicine and critical care, The First Affiliated Hospital of Shandong First Medical University & Shandong Provincial Qianfoshan Hospital,16766 Jingshi Road, Lixia, Jinan, Shandong 250014, P.R. China: C. Zhang <25907623@qq.com> <freezcq66@163.com>

[a] The authors contributed equally

Accepted for publication May 14, 2022

To cite this article: . IL-27 attenuates airway inflammation and epithelial-mesenchymal transition in allergic asthmatic mice possibly via the RhoA/ROCK signalling pathway. *Eur. Cytokine Netw.* 2022; 33(1): 13-24. doi: 10.1684/ecn.2021.0476

ABSTRACT. Background: Asthma is an airway disease characterized by airflow limitation and various additional clinical manifestations. Repeated inflammatory stimulation of the airways leads to epithelial-mesenchymal transition (EMT) which aggravates subepithelial fibrosis during the process of airway remodelling and enhances resistance to corticosteroids and bronchodilators in refractory asthma. There is growing evidence that IL-27 modulates airway remodelling, however, the molecular mechanisms involving IL-27 and EMT are poorly understood. The objective of this study was to investigate the effects of IL-27 on ovalbumin (OVA)-challenged asthmatic mice *in vivo* and TGF-β1-induced EMT in 16HBE cells *in vitro*. **METHODS**: Airway inflammation, mucus secretion, and collagen deposition were analysed by conventional pathological techniques. The ratio of Th17 and Th9 cells in the spleen of mice was measured using flow cytometry, ELISA was performed for cytokine analysis to identify EMT-related molecules and signalling pathways, and other molecular and cellular techniques were used to explore the functional mechanism involving IL-27 and EMT. **RESULTS**: Airway inflammation in asthmatic mice was significantly alleviated by IL-27, with downregulation of RhoA and ROCK, upregulation of E-cadherin, and a decrease of vimentin and α-SMA expression, compared to asthmatic mice. Moreover, the frequency of Th17 and Th9 cells in the spleen of asthmatic mice decreased following treatment with IL-27. In TGF-β1-induced 16HBE cells, the addition of IL-27 was shown to inhibit EMT, based on the expression of E-cadherin, vimentin, and α-SMA. **CONCLUSION**: Intranasal administration of IL-27 attenuates airway inflammation and EMT in a murine model of allergic asthma possibly by downregulating the RhoA/ROCK signalling pathway.

Key words: asthma, airway remodelling, interleukin 27, epithelial-mesenchymal transition, RhoA/ROCK signalling

Asthma is a disease characterized by airflow limitation and various additional clinical manifestations which impose a heavy burden on patients and society as a whole [1]. More specifically, it is characterized by airway inflammation, variable and reversible airflow limitation, and airway hyper-responsiveness (AHR) [2]. Corticosteroids and bronchodilators can alleviate disease symptoms, notably airflow limitation, but they are not effective enough to prevent relapse of the disease [3]. Such relapse, therefore, demonstrates the existence of allergic inflammation or atopy, which is difficult to control, therefore preventing overall development of asthma is challenging. In immunomodulatory disorders, the level of inflammatory factors is increased and this promotes chronic airway inflammation, generating changes in airway structure, such as thickening of the airway wall, subepithelial fibrosis, hypertrophy of smooth muscle cells, and angiogenesis, which are collectively referred to as airway remodelling [4].

Asthma airway remodelling is considered to be the pathological basis of AHR and airway obstruction, which is closely related to clinical prognosis [5]. Thus, there is an urgent need to develop a therapy that targets the biomolecular mechanism involved in airway remodelling.

The continuous airway epithelium is the most significant physical barrier which prevents environmental

doi: 10.1684/ecn.2021.0476

allergens from invading subcutaneous tissue. Compared with healthy individuals, the changes in airway epithelium profile consist of loss of physical barrier function, disruption of tissue homeostasis, and attenuated repair ability [6]. The structural and functional changes in airway epithelial cells are attributed to the pathophysiological process of epithelial-mesenchymal transition (EMT), in which the polarity and tight junctions of epithelial cells degenerate, leading to a mesenchymal cell phenotype, including E-cadherin downregulation and vimentin and α-SMA upregulation [7].

EMT is a process which is involved in the development of embryonic organs, regeneration of damaged tissues, and the phenotypic transformation of tumours. Increasing evidence implies that EMT can occur in the early stage of airway remodelling [8]. The signalling pathway associated with EMT involves TGF-β1. Once cytoplasmic transcription factors are activated, Smads 2/3 are recruited and phosphorylated by TGFβRI on serine residues. The phosphorylated Smad2/3 binds to Smad4 and the complex then translocates to the nucleus to modulate transcription [9-11]. RhoA, a member of the Rho guanosine triphosphatases, acts as a control, to regulate various cell biological functions, including morphology, cytoskeletal motility, differentiation, and growth. ROCK is a downstream signalling molecule of TGF-β1, which is associated with the progression of EMT, and the activation of ROCK leads to the loss of tight junctions between cells [12]. In addition, the RhoA/ROCK signalling pathway is critical in regulating fibrosis of multiple organs, including the lungs, heart, liver, and kidneys [13].

Interleukin (IL) -27 is a member of the IL-6/IL-12 family, produced by dendritic cells, macrophages and activated APCs, and consists of the subunit Epstein Barr virus-induced gene 3 and p28 (IL-27p28) [14]. As a multifunctional immunomodulatory factor, IL-27 exerts various effects on diverse inflammatory diseases including a model for Sjögren syndrome, uveitis, and encephalitis [15, 16]. In addition, the role of IL-27 in regulating airway inflammation and AHR in asthma has been reported [17]. Yoshimoto *et al.* [18] demonstrated that IL-27 decreases the number of Th2 cells and the production of Th2 cytokines by regulating the expression of GATA-3 and T-bet simultaneously in cellular and animal models of allergic inflammation. A previous study showed that IL-27 was critical in promoting Th1 cell differentiation and decreasing Th2 cell number. Preventive intranasal administration of IL-27 was shown to alleviate the development and exacerbation of OVA-challenged mice by impairing STAT1 phosphorylation, relative to the treatment group [19]. In an animal model of allergic asthma, intranasal administration of IL-27 relieved chronic airway inflammation by increasing the ratio of Th1 to T (Treg) cells. In addition, IL-27 increased the levels of C-C motif chemokine ligand 2 (CCL2, CCL3, and CCL4) in HBE cells, triggering monocyte recruitment, and the recruited MPS cells secreted IL-27 in a positive feedback cycle reducing aggregation by airway inflammatory factors [20]. We previously reported that IL-27 suppresses airway remodelling and airway inflammation by upregulating the activation of STAT1 and STAT3 in an experimental model of chronic asthma [21]. However, the precise relationship between IL-27 and asthma is still not clear.

In the present study, the effect of IL-27 on airway inflammation and EMT was investigated *in vivo* using OVA-challenged asthmatic mice, with a view to identifying the signalling pathways involved. Furthermore, we explored the role of IL-27 *in vitro* based on induction of EMT markers in human bronchial epithelial cells (16HBE) stimulated with TGF-β1. Knowledge of the novel mechanisms associated with IL-27 and airway inflammation and EMT in this study may potentially provide a valuable target for the treatment of asthma in the future.

METHODS

Animals

Female BALB/c mice (n=30; weight: 25-28 g; eight weeks old), obtained from the Experimental Animal centre of Shandong University, were maintained in a specific pathogen-free and temperature-controlled room (22±1°C) under 12-hour dark/light cycles, with relative humidity of 55% and ad libitum free access to food and water. Animal procedures were in accordance with the National Institutes of Health Guide for the Care and Use of Laboratory Animals and approved by the First Affiliated Hospital of Shandong, First Medical University & Shandong Provincial Qianfoshan Hospital Ethics committee on Animal care.

Experimental animal protocol

The experimental mice were assigned to three study groups (10 mice per group) randomly: control group (Control), OVA group (OVA), and OVA+IL-27 group (OVA+IL-27). Sensitization and challenge using the mice asthma model were performed by intraperitoneal injection and aerosol inhalation of OVA (Sigma-Aldrich; Merck KGaA) solution using a modified method [22, 23]. The first step was to establish the primary sensitization state of asthmatic mice. On Day 0 and Day 7, the OVA and OVA + IL-27 group of mice were intraperitoneally injected with a mixture containing 20 μg OVA /2 mg Alum (Sigma-Aldrich; Merck KGaA)/200 μL PBS (Invitrogen; Thermo Fisher Scientific), while the control group of mice were administrated with an equal amount of solution containing 2 mg Alum/200 μL PBS. The next step was the induction and maintenance of the asthmatic state from Day 14; the mice in the OVA and OVA + IL-27 groups were treated with 3% OVA solution via ultrasonic atomization/inhalation every day for 30 minutes for three consecutive days. On Days 21 and the following four weeks, the mice inhaled 3% OVA solution three times per week, and the control group of mice inhaled an equal amount of PBS. The mice in the OVA+ IL-27 group were treated intranasally (i.n.) with IL-27 (sc-390482; Santa Cruz Biotechnology, Inc; 50 ng IL-27 in 50 μL PBS/mouse) before the second OVA sensitization, for 14 consecutive days, twice a day. On Days 14-16 and 21-48, the mice were given IL-27 i.n. (20 ng IL-27 in 50 μL PBS/mouse) one hour prior to OVA challenge (*figure 1A*). All of the

mice were euthanized immediately after the assessment of AHR.

Assessment of AHR

The Buxco invasive test system (America) was applied to measure airway reactivity including lung resistance (RL) and dynamic lung compliance (Cdyn), as previously reported [24, 25]. Briefly, mice in each group were anesthetized by intraperitoneal injection of sodium pentobarbital (50 mg/kg). After the skin of the neck was disinfected with 75% alcohol, the trachea was exposed and endotracheal intubation was applied to the Buxco test system, and the auxiliary breathing equipment was connected to the newly placed endotracheal intubation in the closed lung function. Respiratory waveform stability of the mice was closely monitored, and baseline values were recorded when the variation rate of lung resistance values was less than 5% and stabilized for two minutes. Liquid PBS in aerosol with subsequent increasing doses of 3.125, 6.25 and 12.5 mg/mL methacholine (Mch) (Sigma-Aldrich; Merck KGaA) was atomized into the detection device for 10 seconds for each dose, respectively. Airway resistance and dynamic lung compliance were assessed by measuring the percentage increase over baseline value (PBS challenge).

Bronchoalveolar lavage fluid (BALF)

After the last OVA challenge and following the assessment of AHR, all the mice were euthanized by cervical dislocation. BALF, intact spleen and lung tissues were collected for following studies. BALF was collected immediately using sterile ice-cold PBS lavage four times (0.5 mL per time) (to ensure >80% alveolar macrophages). Subsequently, the BALF was centrifuged (1,500g for 5 minutes at 4°C). The supernatant was collected and stored at -80°C until enzyme-linked immunosorbent assays (ELISA) were performed for cytokine detection.

Lung histology

Tissue from the right lung of mice was removed from the chest cavity and fixed in 4% paraformaldehyde for 24 hours. After paraffin embedding, lung samples were then sectioned by microtome into 5-μm-thick slices,

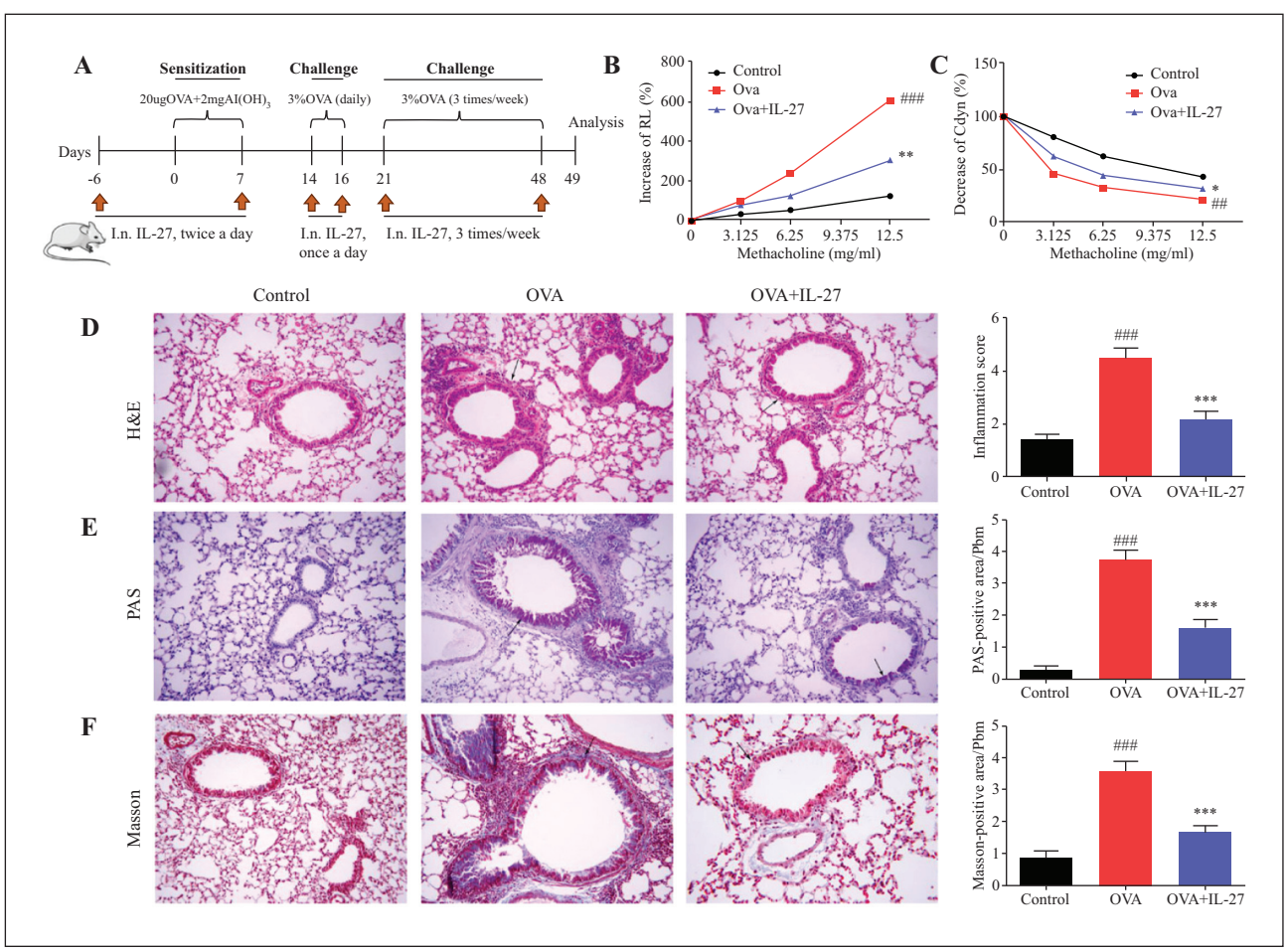

Figure 1

The effect of intranasal administration of IL-27 on Mch-induced AHR in asthmatic mice. **A**) Murine OVA asthma model and schematic diagram of IL-27 administration. **B**, **C**) Buxco system: RL and Cdyn were used to measure airway responsiveness to Mch. **D**) H&E staining to detect aspects of inflammation changes (arrow). Representative photomicrographs from each group are shown (x200 magnification). **E**) Mucus production (arrow) in each group measured by PAS staining. Representative photomicrographs from each group are shown (x200 magnification). **F**) Collagen deposition (arrow) analysed using Masson's trichrome staining. Differences in inflammatory aspects, mucus production and collagen deposition were scored in order to evaluate tissue inflammation (PAS- and Masson-positive areas were calculated; n=10. $^{\#\#}p$<0.01 and $^{\#\#\#}p$<0.001 vs. control group; $^{*}p$<0.05, $^{**}p$<0.01, and $^{***}p$<0.001 vs. OVA group).

dewaxed in xylene, rehydrated in graded ethanol, and stained with haematoxylin and eosin (H&E) in order to assess airway inflammation. Periodic acid-Schiff (PAS) staining was performed for the evaluation of mucus production, and Masson's trichrome for analysis of changes in collagen deposition; all staining procedures were conducted according to a standard protocol [26]. All dye reagents were purchased from Solarbio (Beijing, China). H&E-stained lung sections were observed under a random field of vision using an optical microscope according to a blind method, and airway inflammation was evaluated according to a previously reported method [27, 28]. Three different fields were observed for each section. Areas of collagen fibre beneath the basement membrane were stained blue using Masson's trichrome. Morphometric analysis (Image J 6.0; Media cybernetics) was conducted to measure the perimeter of the basement membrane (Pbm) and Masson-positive area, and the mean value corresponding to the Masson-positive area was divided by the Pbm. Similarly, the bronchioles (1.0-2.0 mm long), with relatively complete epithelial basement membranes, were randomly selected, and the area of goblet cells (stained with amaranth) was analysed using Image J 6.0. The ratio of the area stained with PAS to Pbm was calculated accordingly.

ELISAs

The concentrations of IL-4 (ab100710), IL-13 (ab219634), IFN-γ (ab252363), IL-9 (ab222505) and IL-17A (ab199081) (all from Abcam) in BALF were detected using ELISA kits following the manufacturers' instructions.

Measurement of Th9 and Th17 cells in the spleen

The spleen was harvested and ground with RPMI-1640 media (Invitrogen), and the supernatant was removed, and red blood cell lysis buffer was added for rinsing to obtain a single-cell suspension. DMEM medium (Santa Cruz Biotechnology) was then added to the cell pellet, followed by a leukocyte activation cocktail (No. 550583, BD Biosciences, USA). Subsequently, the cells were stimulated and cultured for five hours. CD4-FITC antibody solution mix (No. 4304296, RM4-5, BD Biosciences, USA) was added, and then the cells were incubated at 4˚C for 30 minutes in the dark. After surface staining, the cells were fixed and permeabilized with BD cytofix/cytoperm kit (No. 4347572, BD Biosciences) at 4°C in the dark for 45 minutes. The cells were washed with 1*Perm Buffer (Santa Cruz Biotechnology) at 400g for 5 minutes. Following washing, the cells were stained intracellularly for anti-IL-9 (ab227037, Abcam) and anti-IL-17A (ab79056, Abcam) antibodies (5 μg/mL, respectively) at 4˚C for 45 minutes. The cells with intracellular staining were washed with 1*Perm Buffer and measured by flow cytometry (C5 Flow Cytometer System).

Reverse transcription-quantitative PCR (RT-qPCR)

RT-qPCR was performed to measure the mRNA levels of E-cadherin, vimentin, and α-SMA. Total RNA from lung tissue was isolated using TRIzol reagent (Invitrogen). RNA concentration and the OD260/OD280 ratio (1.8∼2.0), based on absorbance values at A260 nm and A280 nm using the Nanodrop™ Nd-1000 spectrophotometer (Invitrogen), were measured, and the RNA was used as a template for reverse transcription. Complementary (c)DNA was synthesized using the PrimeScript first-strand cDNA synthesis kit (Invitrogen). Subsequent qPCR was conducted using SYBR green reagent on the ABI 7000 PCR instrument (Thermo Fisher Scientific). The 20-μl PCR reaction mixture consisted of 10 μl SYBR Premix Ex Taq (Solarbio), 2 μl cDNA template, 0.8 μl primer (0.4 μl each forward and reverse) and 7.2 μl dH_2O. The primers used were as follows: E-cadherin, 5′-AAAAGAAGGCTGTCCTTGGC-3′ (forward) and 5′-GAGGTCTACACCTTCCCGGT-3′ (reverse); vimentin, 5′-TCCACTTTCCGTTCA AGGTC-3′ (forward) and 5′-AGAGAGAG-GAAGCCGAAAGC-3′ (reverse); α-SMA, 5′-CGGGACATCAAGGAGAAACT-3′ (forward) and 5′-CCCATCAGGCAACTC GTAA-3′ (reverse). PCR was carried out as follows: initial denaturation at 95˚C for 10 minutes, followed by 40 cycles of 10 seconds at 95˚C and 20 seconds at 50˚C, and a final extension of 25 seconds at 72˚C. The relative mRNA levels were measured using the $2^{-\Delta\Delta Cq}$ method [29]. The data presented correspond to the average of triplicate experiments.

Cell culture and treatment

16HBE cells (FMGBio, Shanghai, China) were cultured in DMEM complete medium (Sigma-Aldrich; Merck KGaA) containing 10% foetal bovine serum (FBS; Hyclone). The cells were grown in a humidified incubator at 37˚C with 5% CO_2. Subculturing was conducted until the cells reached 90% confluence using 0.25% trypsin containing 0.02% EDTA (Sigma-Aldrich; Merck KGaA).

Immunofluorescence

Cells at 80% confluence were starved for 24 hours in culture medium with 1% FBS, and treated daily with IL-27 (15 ng/mL), TGF-β1 (15 ng/mL), or a combination of IL-27 and TGF-β1 (both 15 ng/mL) for 72 hours. The cytokine concentrations and detection time were obtained based on a pilot study. To determine the protein level of E-cadherin, vimentin and α-SMA, cells in culture dishes were fixed with 4% paraformaldehyde and permeabilized with PBS containing 0.1% Triton X-100 for 10 minutes. The sample was incubated with secondary antibody (1:1,000; sc-2018; Santa Cruz Biotechnology) for 2 hours at 22±2˚C, and then 16HBE cells were blocked with primary antibodies against E-cadherin (1:50; cat. no. sc-8426), vimentin (1:100; cat. no. sc-6260) and α-SMA (1:50; cat. no. sc-53142; Santa Cruz Biotechnology), respectively, overnight at 4˚C. The cells were then stained with FITC-conjugated mouse anti-rabbit IgG (sc-2359; Santa Cruz Biotechnology) for one hour at 22±2˚C. DAPI (Beyotime) was used to stain nuclei before acquiring images. A positive antibody response was measured by

fluorescence microscopy (Olympus, Tokyo, Japan), and the labelled fields of each section were analysed using Image-pro plus (Media Cybernetics, Rockville, MD, USA).

Migration assays

Transwell migration was conducted to evaluate the migrating ability of 16HBE cells. Cells were seeded into the upper chamber of transwell plates (EMD Millipore) and maintained in 100 μL serum-free medium. In addition, the lower chamber was filled with 600 μL complete medium. TGF-β1 (15 ng/mL) or/and IL-27 (15 ng/mL) was added to the upper chamber for the experimental groups, and no reagent was added for the control group. Following 72 hours of incubation at 37˚C, the cells in the upper side were wiped off using a clean cotton swab, and traversed cells in the lower chambers were fixed with 4% paraformaldehyde for 20 minutes, followed by staining with 0.1% crystal violet (Beyotime) for 10 minutes at 22±2˚C. Five visual fields were randomly selected for counting the migrated cells using an inverted microscope (Olympus, Tokyo, Japan) at 200x magnification.

Western blotting

Total protein was extracted immediately from lung tissues and 16HBE cells using ice-cold RIPA buffer (cat. no. P0013K; Beyotime) for 30 minutes. The protein concentration of the samples from the 16HBE cells and the BALB/c mice was assessed using the BCA kit (cat. no. P0010; Beyotime). Briefly, 30 μg proteins of each sample were loaded on to a 10% SDS acrylamide gel and the separated proteins were transferred onto polyvinylidene difluoride membranes (Thermo Fisher Scientific). After blocking with 5% non-fat dried milk for one hour at 22±2˚C, the membranes were incubated overnight at 4˚C with primary antibodies against E-cadherin (1:1000; ab7319), vimentin (1:1000; ab92547), α-SMA (1:2000; ab5694), RhoA (1:1000; ab187027), ROCK1 (1:1000; ab245369) and GAPDH (1:1000; ab8245; Abcam). After three washes with Tris-buffered saline containing Tween-20 (TBST), horseradish peroxidase-conjugated anti-rabbit IgG (sc-2004; 1:4000; Santa Cruz Biotechnology) was used for membrane incubation at 22±2˚C for one hour. Bands were visualized using ECL reagent kit (Solarbio Science & Technology, Beijing, China). Protein quantification was performed using Image Pro Plus 6.0. The relative expression of target proteins to GAPDH was calculated.

Statistical analysis

SPSS version 25.0 (SPSS, Inc., Chicago, IL, USA) was used for statistical analysis. The results are expressed as mean ± standard deviation (SD). One-way analysis of variance (ANOVA) followed by a Dunnett's test was used to compare differences between multiple groups. Significant differences were considered at $p<0.05$.

RESULTS

Effect of intranasal administration of IL-27 on Mch-induced AHR in asthmatic mice

To observe the effects of IL-27 on asthma, OVA-challenged asthmatic mice were used (*figure 1A*). AHR, a hall mark of asthma, was analysed to measure RL and Cdyn when stimulated with the different concentrations of Mch (*figure 1B, C*). No significant differences among the three groups at baseline (PBS challenge) were observed. Airway responsiveness to Mch was significantly elevated in OVA-challenged mice, as evidenced by the observed increase in RL and decrease in Cdyn compared to mice in the control group ($p<0.05$). Administration of IL-27 in the OVA +IL-27 group of mice led to a significant decrease in RL and increase in Cdyn, compared to the OVA group of mice ($p<0.05$).

To evaluate the effects of IL-27 on pathological features of airway remodelling, histological examination was performed. OVA challenge resulted in conspicuous infiltration of inflammatory cells, mucus production and subepithelial collagen deposition in the tracheobronchial mucosa and airway lumen. In contrast to the OVA group, in the OVA + IL-27 group, intranasal administration of IL-27 significantly inhibited the infiltration of inflammatory cells around bronchi ($p<0.05$) (*figure 1D*), mucus production ($p<0.05$) (*figure 1E*) and collagen deposition ($p<0.05$) (*figure 1F*). These data collectively show that intranasal administration of IL-27 was effective in preventing airway remodelling in the murine OVA asthma model.

Effect of intranasal administration of IL-27 on cytokine levels and Th9/Th17 cells in asthmatic mice

The release of Th2 cytokines is one of the main characteristics of allergic airway inflammation. IL-9 is involved in the pathogenesis of asthma as it promotes the production of Th2 cytokines, mucus hypersecretion, and accumulation of eosinophils. IL-17A can accelerate the imbalance of the Th1/Th2 ratio which contributes to acute AHR and airway inflammation. To investigate whether IL-27 attenuates airway inflammation by affecting the levels of cytokines mentioned above, cytokine levels in BALF were evaluated in our mouse model. Th2 cytokines (IL-4 and IL-13) (*figure 2B*), IL-9 (*figure 2D*) and IL-17A (*figure 2E*) were upregulated in the OVA group, while IFN-γ (*figure 2C*) was downregulated, as compared with control group ($p<0.05$). Interestingly, intranasal administration of IL-27 significantly decreased IL-4, IL-13, IL-9, and IL-17A levels, and significantly elevated IFN-γ level, compared to the OVA group ($p<0.05$).

It is generally accepted that disruption of the balance of Th1/Th2 cells is an important mechanism in the occurrence and development of asthma. However, clinical and experimental research have shown that the pathogenesis of asthma is complex, involving not only the imbalance of Th1/Th2, but also changes in the proportion of Th9 and Th17 cells. As we observed a decrease in IL-9 and IL-17A levels in BALF samples

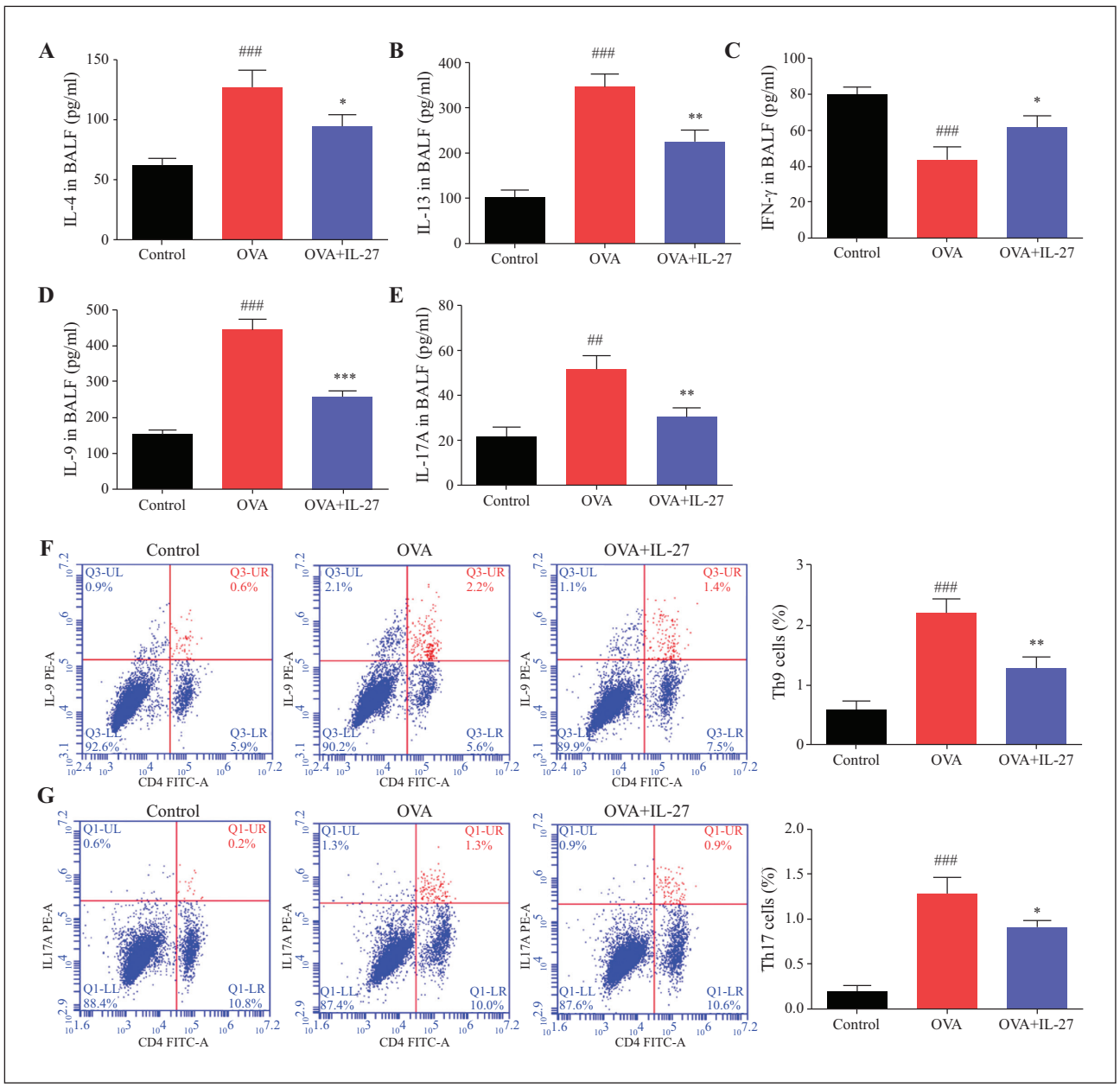

Figure 2

The effect of intranasal administration of IL-27 on the level of cytokines and Th9 and Th17 cells in OVA-challenged asthmatic mice. The concentrations of IL-4 (**A**), IL-13 (**B**), IFN-γ (**C**), IL-9 (**D**), and IL-17A (**E**) in BALF samples were detected using ELISAs. The percentages of Th9+ (**F**) and Th17+ (**G**) cells in CD4+ T cells in the spleen were detected using flow cytometry (n=10; $^{\#\#}p$<0.01 and $^{\#\#\#}p$<0.001 vs. control group; $^{*}p$<0.05, $^{**}p$<0.01, and $^{***}p$<0.001 vs. OVA group).

from IL-27-treated asthmatic mice, we further measured the level of Th9 and Th17 cells in the spleen. Th9 (*figure 2F*) and Th17 (*figure 2G*) cells increased significantly in the murine OVA asthma model, compared to the control group, however, intranasal administration of IL-27 significantly restored the levels of Th9 and Th17 cells (p<0.05) (*figure 2F* and *2G*, respectively).

Effect of intranasal administration of IL-27 on EMT in asthmatic mice

The mRNA levels of the EMT biomarkers (E-cadherin, α-SMA, and vimentin) were measured in tissue of asthmatic mice to confirm the effects of IL-27. In OVA-challenged asthmatic mice, mRNA of the epithelial cell marker, E-cadherin, was downregulated (p<0.05) (*figure 3A*), whereas mRNA levels of the mesenchymal markers, α-SMA (p<0.05) (*figure 3B*) and vimentin (p<0.05) (*figure 3C*), were upregulated, compared to control mice. After intranasal administration of IL-27, the mRNA level of E-cadherin was upregulated, and the mRNA levels of vimentin and α-SMA were downregulated, compared to the OVA group (p<0.05). Furthermore, the protein levels of E-cadherin, vimentin, and α-SMA, analysed using western blotting, showed the same results as above. These results collectively indicate that IL-27 is critical in EMT in this murine model of asthma.

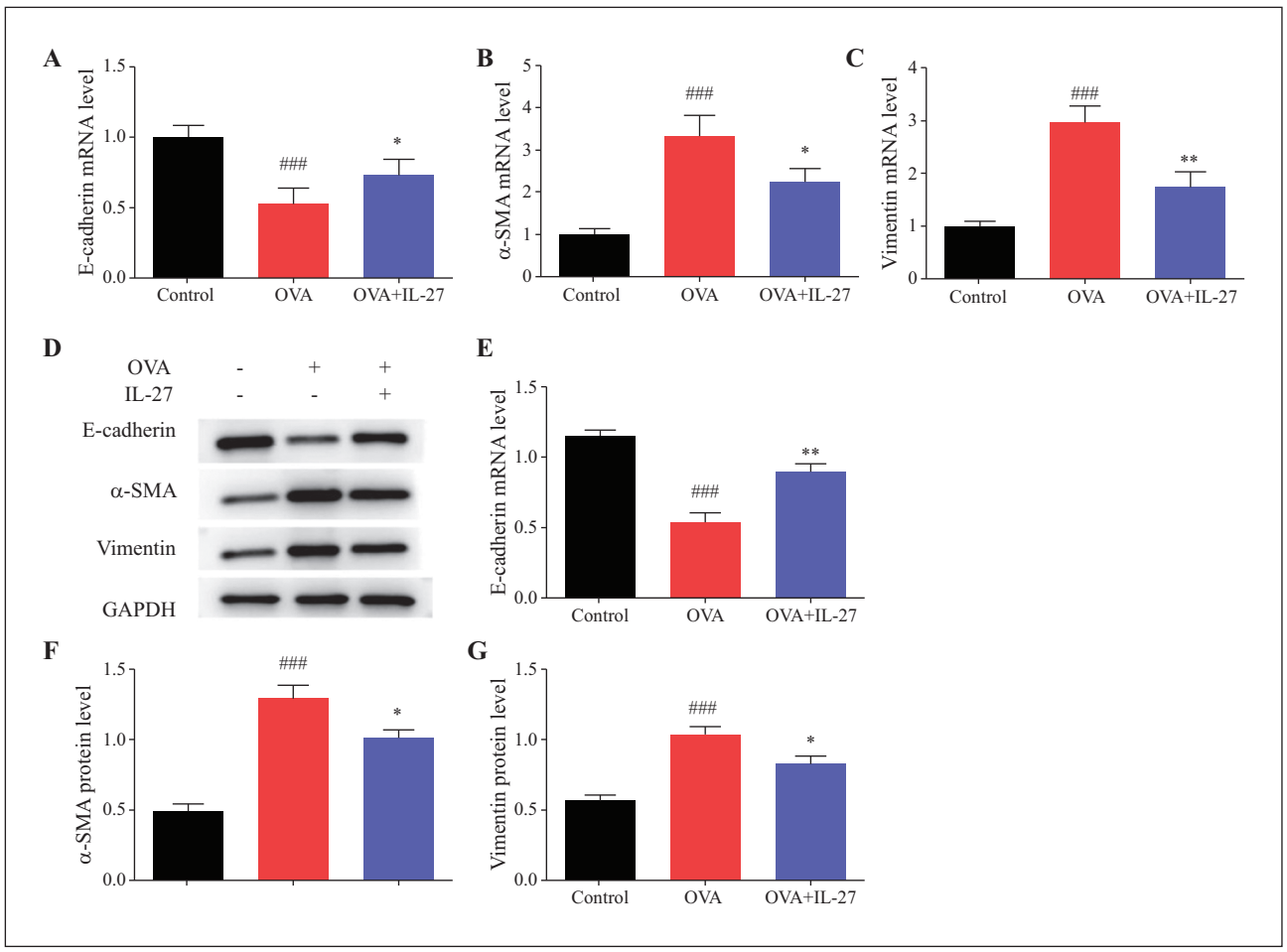

Figure 3

The effect of IL-27 *in vivo* on EMT biomarkers in OVA-challenged asthmatic mice. The mRNA levels of E-cadherin (**A**), α-SMA (**B**), and vimentin (**C**) in mouse lung tissues were detected using RT-qPCR. **D**) Immunoblots for protein expression levels in lung tissue, with quantification: E-cadherin (**E**), α-SMA (**F**), and vimentin (**G**). The graphs display the average of triplicate experiments ($^{###}p<0.001$ vs. control group; $^{*}p<0.05$ and $^{**}p<0.01$ vs. OVA group).

Effect of IL-27 on TGF-β1-induced EMT markers and migration in vitro

To explore the effects of IL-27 on EMT markers, 16HBE cells were treated *in vitro* with IL-27, TGF-β1 or a combination of IL-27 and TGF-β1, and the expression of the EMT biomarkers was examined by immunofluorescence. As expected, TGF-β1 stimulation of 16HBE cells led to a remarkable decrease in E-cadherin ($p<0.05$) (*figure 4A*) and increase in α-SMA ($p<0.05$) (*figure 4B*) and vimentin ($p<0.05$) (*figure 4C*), compared to control and IL-27 groups. However, in the presence of a combination of IL-27 and TGF-β1, E-cadherin increased and vimentin and α-SMA decreased ($p<0.05$). These results suggest that IL-27 inhibited TGF-β1-induced EMT changes in 16HBE cells, including loss of the epithelial phenotype and acquisition of a mesenchymal phenotype in these bronchial epithelial cells, subsequently inducing their ability to migrate.

In order to evaluate the effect of IL-27 on migration of 16HBE cells, the transwell migration assay was performed (*figure 5*). Results indicated that the migration of 16HBE cells was increased by TGF-β1, compared to the control group ($p<0.05$) (*figure 5A, B*). Following treatment with IL-27, migration of TGF-β1-treated 16HBE cells was repressed ($p<0.05$).

Effect of IL-27 on RhoA and ROCK expression in vivo and in vitro

To investigate the signalling pathways triggered by IL-27, which may be involved in regulating the pathogenesis of asthma, RhoA and ROCK1 expression was measured in mice and 16HBE cells. As shown in *figure 6*, RhoA ($p<0.05$) (*figure 6A, B*) and ROCK1 ($p<0.05$) (*figure 6A, C*) protein levels were significantly increased in the lung tissues of OVA-challenged mice compared to lung tissue of control mice. In contrast, in IL-27-treated asthmatic mice, lower protein levels of RhoA and ROCK1 were observed.

To further investigate the role of IL-27 in regulating RhoA/ROCK signalling, complementary *in vitro* studies were carried out using the 16HBE cell line. The levels of RhoA ($p<0.05$) (*figure 6D, E*) and ROCK1 ($p<0.05$) (*figure 6D, F*) were increased significantly in TGF-β1-treated 16HBE cells. However, treatment with IL-27 decreased the expression of RhoA and ROCK1 in TGF-β1-treated 16HBE cells ($p<0.05$).

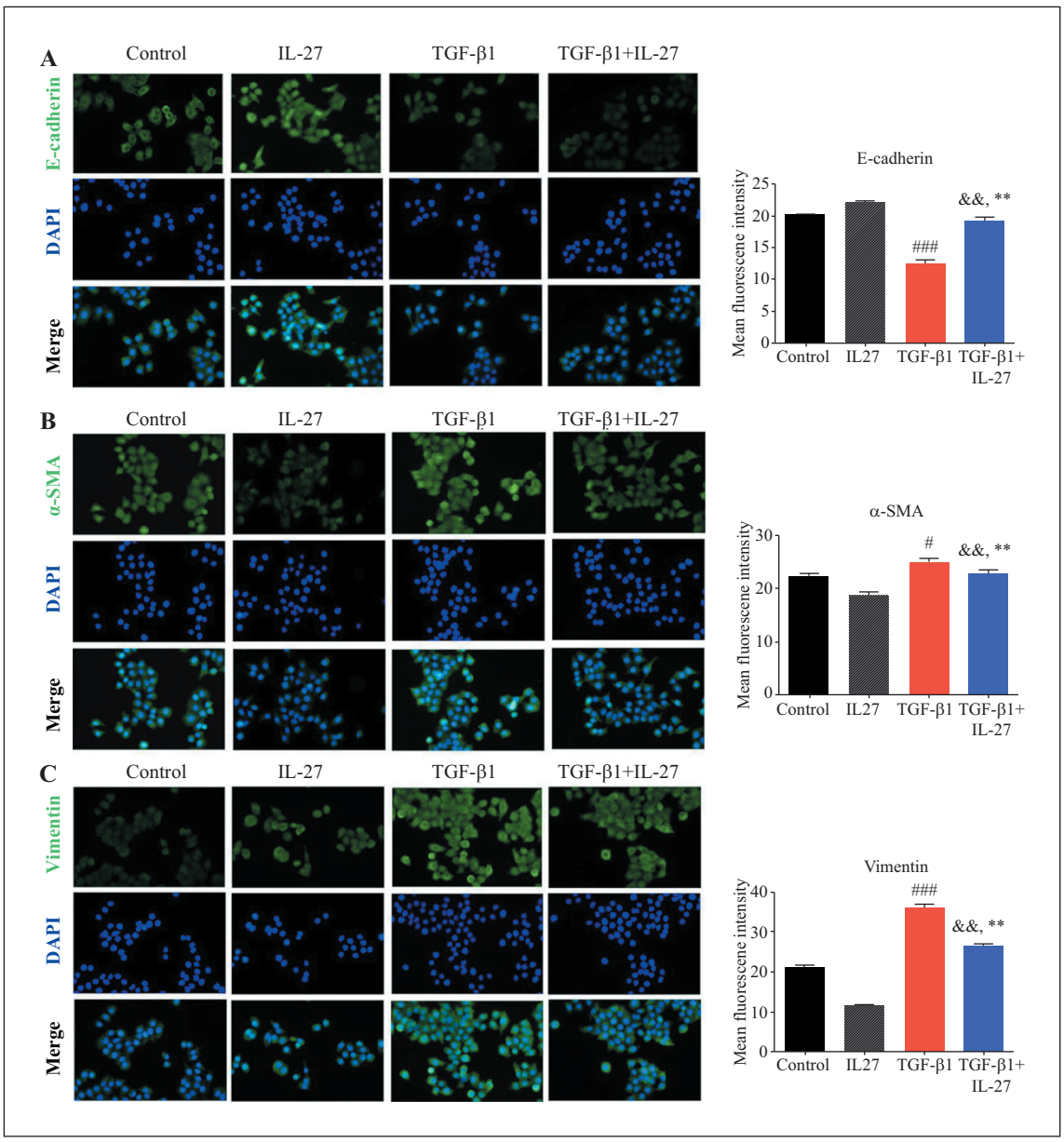

Figure 4

The effect of IL-27 on TGF-β1-induced EMT expression markers in 16HBE cells *in vitro*. The expression of E-cadherin (**A**), α-SMA (**B**), and vimentin (**C**) was determined by immunofluorescence, and representative images are presented (x200 magnification; scale bars=100 μm). Target proteins are stained green and cell nuclei are stained blue. The levels of E-cadherin, α-SMA, and vimentin were calculated using Image-Pro Plus 6.0. The graphs display the average of triplicate experiments ($^{\#}p<0.05$ and $^{\#\#\#}p<0.001$ vs. control group; $^{**}p<0.01$ vs. TGF-β1 group, $^{\&\&}p<0.01$ vs. IL-27 group).

DISCUSSION

The present study shows that intranasal administration of IL-27 significantly suppressed airway inflammation and EMT in a mouse model of asthma *in vivo*. In addition, our present study establishes that IL-27 inhibited TGF-β1-induced EMT and migration of 16HBE cells *in vitro*. These findings are in line with a previously reported article [20], in which preventative tracheal administration of IL-27 was found to have beneficial effects as treatment for allergic asthma by regulating the lung Th1 microenvironment and inhibition of EMT, and migration of 16HBE cells *in vitro*. Our data suggest that administration of IL-27 may attenuate airway inflammation and EMT via regulation of the RhoA/ROCK signalling pathway.

IL-27 is a pleiotropic cytokine which is involved in the immune response of different autoimmune and inflammatory diseases [30]. Current studies have shown that IL-27 is critical in suppressing differentiation of naïve CD4+ T cells into Th2 cells and alleviating airway inflammation in an asthma mouse model [31]. Th2 cells are involved in the pathophysiology of allergic asthma, and the cytokines secreted by Th2 cells are the basis of chronic airway inflammation and AHR. Chronic airway inflammation leads to rearrangement of epithelial cells, resulting in airway resistance and decreased airway compliance. IL-27 can

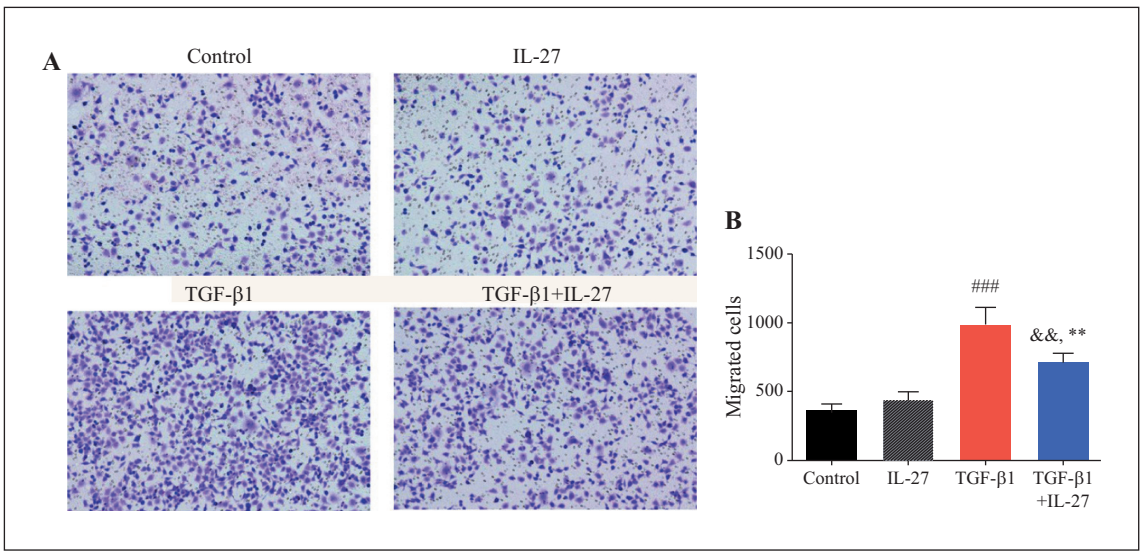

Figure 5
IL-27 inhibited migration of 16HBE cells *in vitro*. Cell migration was measured based on a transwell assay. **A**) Representative images of crystal violet-stained migratory cells (x200 magnification). **B**) Quantification based on the average of triplicate experiments ($^{###}p<0.001$ vs. control group; $^{**}p<0.01$ vs. TGF-β1 group; $^{\&\&}p<0.01$ vs. IL-27 group).

activate T-bet and ICAM-1/LFA-1-dependent pathways in naive CD4+T cells, leading to up-regulation of Th1 differentiation and IFN-γ production [32]. In addition, IL-27 downregulates GATA-3 expression to inhibit Th2 cell proliferation and Th2 cytokine production by regulating the STAT1 signalling pathway [18]. According to previous studies, the accumulation of IL-4, IL-5, and IL-13 in the airway aggravates the infiltration of inflammatory cells, resulting in AHR and obstructive pulmonary ventilation dysfunction [33, 34]. In our study, airway inflammation and AHR in response to Mch was observed in a murine OVA asthma model; intranasal administration of IL-27 suppressed airway inflammation and reversed Mch-induced AHR. Furthermore, Th2 cytokine (IL-4 and IL-13) levels in bronchoalveolar lavage fluid were decreased, and Th1 cytokine (IFN-γ) level was increased in response to IL-27 administration. These studies are consistent with previous research on IL-27 [21].

The Th1/Th2 paradigm is not the only pathogenic feature of asthma, and in recent studies, the role of Th9

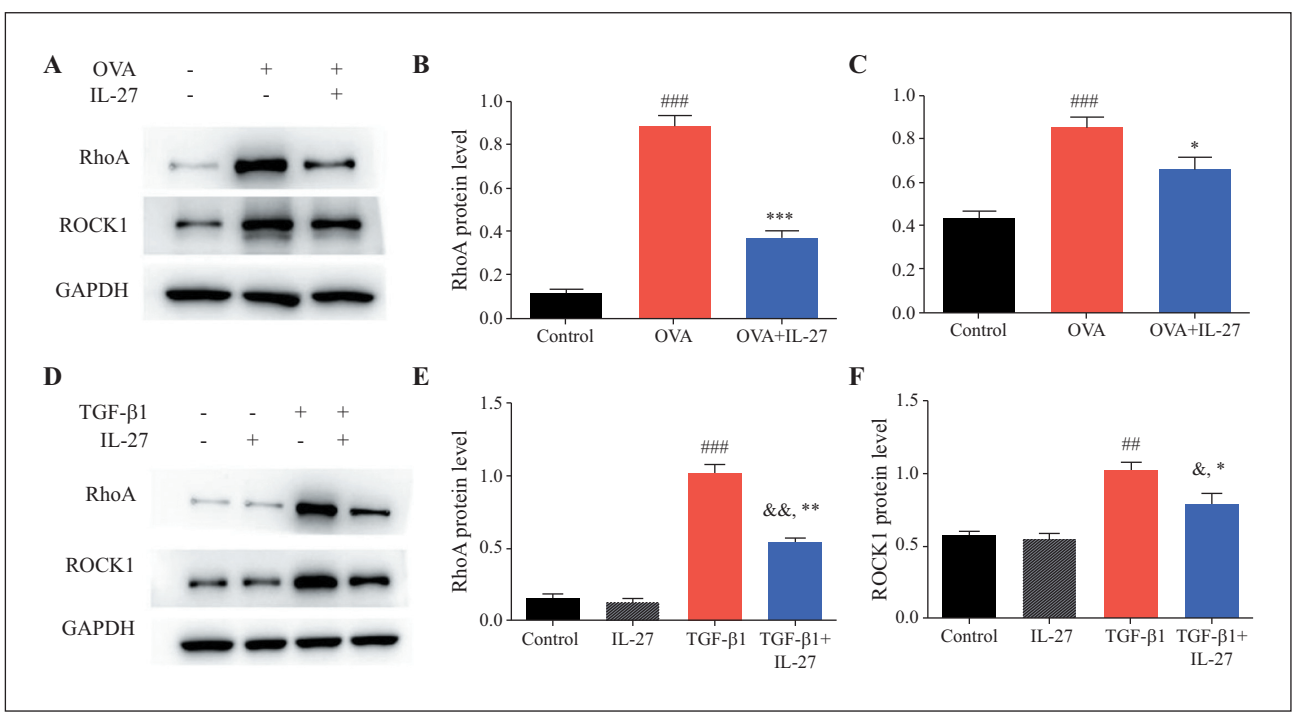

Figure 6
The effect of IL-27 *in vivo* on the RhoA/ROCK signalling pathway in OVA-challenged asthmatic mice (**A-C**), and the effect of IL-27 *in vitro* on TGF-β1-treated 16HBE cells (**D-F**). **A**) Immunoblots for protein expression in lung tissue, with quantitative analysis for RhoA (**B**) and ROCK1 (**C**). **D**) Immunoblots for protein expression in 16HBE cells, with quantitative analysis for RhoA (**E**) and ROCK1 (**F**). The graphs display the average of triplicate experiments ($^{##}p<0.01$ and $^{###}p<0.001$ vs. control group; $^{*}p<0.05$, $^{**}p<0.01$, and $^{***}p<0.001$ vs. OVA or TGF-β1 groups; $^{\&}p<0.05$ and $^{\&\&}p<0.01$ vs. IL-27 group).

and Th17 cells has been expanded [35, 36]. Increased IL-9 is observed in the lungs of asthmatic mice [37]. Functionally, IL-9 was shown to elicit eosinophil-independent bronchial AHR in mice and enhance the release of Th2 cytokines such as IL-4 [38, 39]. Th9 cells are involved in allergic responses by affecting neutrophil aggregation and activation of mast cells in the lung [40]. IL-17 mediates infiltration of neutrophils, leading to excessive mucus production and severe airway remodelling [41, 42]. The number of Th17 cells and serum IL-17 level was shown to control glucocorticoid resistance and airway obstruction in severe asthma [43]. IL-9 and IL-17, to some extent, complement the pathological mechanism of airway inflammation and airway remodelling in asthma. Our data highlight that IL-27 significantly decreased the levels of IL-9 and IL-17, indicating its potential in regulating asthma inflammation. IL-9 and IL-17 are mainly produced by Th9 and Th17 cells, respectively, which prompted us to further measure Th9 and Th17 cells by flow cytometry analysis. As T cell subsets in lung tissue can migrate from the spleen [44, 45], we focused on the proportion of T lymphocytes in this immune organ. In the present study, IL-27 significantly inhibited the level of Th9 and Th17 cells in OVA-induced asthmatic mice, suggesting that IL-27 shows anti-asthmatic effects by controlling Th9 and Th17 cell differentiation.

Airway remodelling is a key feature of asthma pathophysiology and is considered to be the major factor in severe steroid-refractory asthma [46, 47]. Our results show that IL-27 in the OVA mice significantly reduced the degree of subepithelial collagen deposition and goblet cell hyperplasia in the tracheobronchial mucosa and airway lumen, in contrast to OVA mice, indicating that airway remodelling was attenuated by IL-27. EMT is closely involved in the pathophysiology of airway remodelling in asthma, and mounting evidence has revealed that inhibition of EMT can effectively inhibit airway remodelling in asthma [48, 49]. Broadly speaking, EMT can be classified into three categories: type 1 EMT occurs during embryogenesis and is involved in tissue and organ formation; type 2 EMT is related to inflammatory injury, repeated damage and repair, eventually leading to organ fibrosis and destruction; and type 3 EMT occurs in epithelial cancer cells and is associated with the invasion and metastasis of cancer cells [50, 51]. Accumulating evidence indicates that chronic airway inflammatory diseases are mainly associated with type 2 EMT [52]. The respiratory epithelium constitutes a physical barrier that modulates the innate immune response and adaptive immune response. In allergic asthma, airway epithelial cells are stimulated by allergens and inflammatory mediators, which induce damage of the airway epithelial barrier and proliferation of fibroblasts and myofibroblasts [53]. EMT is identified as a process during which epithelial cells are stimulated to gradually lose their epithelial phenotype and acquire mesenchymal characteristics [54]. The accumulation of myofibroblasts and fibroblasts is responsible for the accumulation of excessive extracellular matrix (EMC), which deposits around the bronchial wall, leading to subepithelial fibrosis and airway remodelling. Collagen is also a component of the EMC, and changes in collagen deposition may be analysed with Masson's trichrome. In this study, areas stained with Masson's trichrome were significantly decreased with IL-27 in the OVA-induced asthmatic mice, suggesting that IL-27 may be involved in attenuating airway remodelling by affecting the pathological changes associated with EMT. E-cadherin, vimentin, and α-SMA proteins are considered to be typical biomarkers of EMT. The loss of E-cadherin and increase in vimentin and α-SMA disrupt the structural stability and polarity of epithelial cells, which are subsequently transformed into spindle-shaped cells and migrate. In the OVA-induced asthma mouse model, E-cadherin was found to be down-regulated, and vimentin upregulated [55]. Moreover, the expression of E-cadherin was decreased, whereas fibroblast specific protein 1 and vimentin were increased in OVA-challenged mice [48]. In this study, the expression of EMT-related markers (E-cadherin, vimentin, and α-SMA) was assessed. Our data shows that E-cadherin decreased, and vimentin and α-SMA levels increased in the lung tissues of the asthma group, indicating the occurrence of EMT in asthma, which is consistent with EMT progression reported in previous studies. Furthermore, the present results also demonstrate the suppressive effects of IL-27 on EMT in allergic asthma by further inhibiting vimentin and α-SMA and enhancing E-cadherin.

To further define the mechanisms of IL-27 underlying the observed effects of EMT, a cellular model of bronchial EMT was applied. The ability to induce an epithelial to mesenchymal phenotype in epithelial cells is widely established, and in the present study, TGF-β1 was selected to investigate the role of IL-27 in EMT *in vitro*. Our results show that TGF-β1 inhibited the level of E-cadherin and increased vimentin and α-SMA levels in 16HBE cells, as observed by immunofluorescence. Conversely, these effects were reversed by IL-27. TGF-β1 induces EMT in epithelial cells by inhibiting the expression of tight junction proteins and mesenchymal markers, following enhanced migration [56]. In addition, our research shows that IL-27 may exert antimigration effects on TGF-β1-induced 16HBE cells. This finding is consistent with the evidence of TGF-β1-induced EMT in various cancer cells, including A549, renal, and gastric cancer cells. Thus, it can be concluded that IL-27 inhibits EMT *in vitro* [57].

According to previous results, the complexity of EMT is mediated via regulation of diverse signalling pathways. Cell–cell or cell–ECM interactions can be disrupted by different signalling factors, thereby triggering EMT. Upregulation of SIRT6 has been shown to primarily alleviate EMT through TGF-β1/Smad3 and c-Jun signalling in asthma models [58]. Our previous studies showed that IL-27 exerts anti-airway inflammatory effects through PI3K/Akt and STAT1/3 signalling pathways, however, inhibition of either signal pathway could not completely reverse this phenomenon [17]. IL-27 may affect asthma by triggering more complex multiple signalling cascades, which prompted us to further explore its underlying mechanism. A previous study disclosed that progression of TGF-β1-induced EMT, cytoskeletal reorganization as well as increased expression of α-SMA are regulated through RhoA/ROCK signalling in epitheli-

al cells *in vitro* [59]. Emerging data have confirmed that RhoA is activated by TGF-β1, and is an important molecule that modulates internal structure and the fate of cells via TGF-β1-induced EMT [12]. Regarding asthma, RhoA/ROCK signalling regulates the recruitment of eosinophils to control allergic airway inflammation, whilst an inhibitor of ROCK (Y-27632) was shown to be effective in enhancing substantial changes of the airway smooth muscle cell cytoskeleton in the progression of asthmatic airway remodelling [60]. Consequently, this study demonstrates that the RhoA/ROCK pathway may be involved in OVA-challenged asthmatic mice, and that IL-27 suppresses RhoA and ROCK1 expression and attenuates EMT and airway inflammation. Moreover, *in vitro* studies performed in 16HBE cells indicate the involvement of the RhoA/ROCK signalling pathway in response to TGF-β1, which may induce EMT via reduced E-cadherin expression and increased vimentin and α-SMA expression. Treating 16HBE cells with IL-27 effectively reduces EMT possibly via the RhoA/ROCK signalling pathway.

IL-27 has previously been shown to be involved in regulating human non-small cell lung cancer cell migration [61]. Interestingly, in our study, IL-27 blocked TGF-β1-induced migration of 16HBE cells. These data are in line with a previous study in which IL-27 was reported to be an inhibitor of cell motility and migration [62]. Collectively, our data support the notion that IL-27 inhibits EMT through the RhoA/ROCK signalling pathway by regulating the expression of E-cadherin, α-SMA and vimentin.

CONCLUSIONS

To summarize, we demonstrate the effect of IL-27 on airway inflammation and EMT in asthmatic mice *in vivo* and 16HBE cells *in vitro*. Our current study provides evidence, and highlights the potential of IL-27 in alleviating bronchial EMT via the RhoA/ROCK signalling pathway. These findings provide a novel insight into potential therapeutic strategies to treat asthma.

Disclosure. Financial support: The present study was supported by the Traditional Chinese Medicine Science and Technology development plan project of Shandong Province, China (grant no.2019-0231) and Key research and development plan of Shandong Province, China (grant no.2015GSF121033).
Conflict of interest: none.

REFERENCES

1. Chung KF. Clinical management of severe therapy-resistant asthma. *Expert Rev Respir Med* 2017; 11(5):395-402.
2. Huang C, Zhang Z, Wang L, Liu J, Gong X, Zhang C. ML-7 attenuates airway inflammation and remodeling *via* inhibiting the secretion of Th2 cytokines in mice model of asthma. *Mol Med Rep* 2018; 17(5):6293-300.
3. Pike KC, Levy ML, Moreiras J, Fleming L. Managing problematic severe asthma: beyond the guidelines. *Arch Dis Child* 2018; 103(4):392-7.
4. Dong L, Wang Y, Zheng T, *et al*. Hypoxic hUCMSC-derived extracellular vesicles attenuate allergic airway inflammation and airway remodeling in chronic asthma mice. *Stem Cell Res Ther* 2021; 12(1):4.
5. Deng Z, Xie H, Cheng W, *et al*. Dabigatran ameliorates airway smooth muscle remodeling in asthma by modulating Yes-associated protein. *J Cell Mol Med* 2020; 24(14):8179-93.
6. Hackett TL, Warner SM, Stefanowicz D, *et al*. Induction of epithelial-mesenchymal transition in primary airway epithelial cells from patients with asthma by transforming growth factor-beta1. *Am J Respir Crit Care Med* 2009; 180(2):122-33.
7. Hackett TL. Epithelial-mesenchymal transition in the pathophysiology of airway remodelling in asthma. *Curr Opin Allergy Clin Immunol* 2012; 12(1):53-9.
8. Kalluri R. EMT: when epithelial cells decide to become mesenchymal-like cells. *J Clin Invest* 2009; 119(6):1417-9.
9. Chang X, Tian M, Zhang Q, Gao J, Li S, Sun Y. Nano nickel oxide promotes epithelial-mesenchymal transition through transforming growth factor β1/smads signaling pathway in A549 cells. *Environ Toxicol* 2020; 35(12):1308-17.
10. Hujie G, Zhou SH, Zhang H, *et al*. MicroRNA-10b regulates epithelial-mesenchymal transition by modulating KLF4/KLF11/Smads in hepatocellular carcinoma. *Cancer Cell Int* 2018; 18 : 10.
11. Wang Z, Wang L, Shi B, *et al*. Demethyleneberberine promotes apoptosis and suppresses TGF-β/Smads induced EMT in the colon cancer cells HCT-116. *Cell Biochem Funct* 2021; 39(6):763-70.
12. Zhang K, Zhang H, Xiang H, *et al*. TGF-β1 induces the dissolution of tight junctions in human renal proximal tubular cells: role of the RhoA/ROCK signaling pathway. *Int J Mol Med* 2013; 32(2):464-8.
13. Shi Z, Wang Q, Zhang Y, Jiang D. Extracellular vesicles produced by bone marrow mesenchymal stem cells attenuate renal fibrosis, in part by inhibiting the RhoA/ROCK pathway, in a UUO rat model. *Stem Cell Res Ther* 2020; 11(1):253.
14. Bosmann M, Strobl B, Kichler N, *et al*. Tyrosine kinase 2 promotes sepsis-associated lethality by facilitating production of interleukin-27. *J Leukoc Biol* 2014; 96(1):123-31.
15. Choi JK, Yu CR. IL-27-producing B-1a cells suppress neuroinflammation and CNS autoimmune diseases. *Proc Natl Acad Sci U S A* 2021; 118(47):e2109548118.
16. Qi J, Zhang Z, Tang X, Li W, Chen W, Yao G. IL-27 regulated CD4(+)IL-10(+) T cells in experimental Sjögren syndrome. *Front Immunol* 2020; 11 : 1699.
17. Li X, Zhou L, Zhang Z, Liu Y, Liu J, Zhang C. IL-27 alleviates airway remodeling in a mouse model of asthma *via* PI3K/Akt pathway. *Exp Lung Res* 2020; 46(3-4):98-108.
18. Yoshimoto T, Yoshimoto T, Yasuda K, Mizuguchi J, Nakanishi K. IL-27 suppresses Th2 cell development and Th2 cytokines production from polarized Th2 cells: a novel therapeutic way for Th2-mediated allergic inflammation. *J Immunol* 2007; 179 (7):4415-23.
19. Su X, Pan J, Bai F, *et al*. IL-27 attenuates airway inflammation in a mouse asthma model via the STAT1 and GADD45γ/p38 MAPK pathways. *J Transl Med* 2016; 14(1):283.
20. Liu X, Li S, Jin J, *et al*. Preventative tracheal administration of interleukin-27 attenuates allergic asthma by improving the lung Th1 microenvironment. *J Cell Physiol* 2019; 234(5):6642-53.
21. Lu D, Lu J, Ji X, *et al*. IL-27 suppresses airway inflammation, hyperresponsiveness and remodeling *via* the STAT1 and STAT3 pathways in mice with allergic asthma. *Int J Mol Med* 2020; 46 (2):641-52.
22. Yu QL, Chen Z. Establishment of different experimental asthma models in mice. *Exp Ther Med* 2018; 15(3):2492-8.
23. Zosky GR, Sly PD. Animal models of asthma. *Clin Exp Allergy* 2007; 37(7):973-88.
24. Hoymann HG. Lung function measurements in rodents in safety pharmacology studies. *Front Pharmacol* 2012; 3 : 156.

25. Wei Y, Luo QL, Sun J, Chen MX, Liu F, Dong JC. Bu-Shen-Yi-Qi formulae suppress chronic airway inflammation and regulate Th17/Treg imbalance in the murine ovalbumin asthma model. *J Ethnopharmacol* 2015; 164 : 368-77.
26. Duan L, Li J, Ma P, Yang X, Xu S. Vitamin E antagonizes ozone-induced asthma exacerbation in Balb/c mice through the Nrf2 pathway. *Food Chem Toxicol* 2017; 107(Pt A):47-56.
27. Balkrishna A, Solleti SK, Singh H, *et al*. Herbal decoction Divya-Swasari-Kwath attenuates airway inflammation and remodeling through Nrf-2 mediated antioxidant lung defence in mouse model of allergic asthma. *Phytomedicine* 2020; 78 : 153295.
28. Liu Y, Zhang H, Ni R, Jia WQ, Wang YY. IL-4R suppresses airway inflammation in bronchial asthma by inhibiting the IL-4/STAT6 pathway. *Pulm Pharmacol Ther* 2017; 43 : 32-8.
29. Skrzypski M. Quantitative reverse transcriptase real-time polymerase chain reaction (qRT-PCR) in translational oncology: lung cancer perspective. *Lung Cancer* 2008; 59(2):147-54.
30. Thomé R, Moore JN, Mari ER, *et al*. Induction of peripheral tolerance in ongoing autoimmune inflammation requires interleukin 27 signaling in dendritic cells. *Front Immunol* 2017; 8 : 1392.
31. Chen Z, Wang S, Erekosima N, *et al*. IL-4 confers resistance to IL-27-mediated suppression on CD4+ T cells by impairing signal transducer and activator of transcription 1 signaling. *J Allergy Clin Immunol* 2013; 132(4):912-21.e1-5.
32. Shibata S, Tada Y, Asano Y, *et al*. IL-27 activates Th1-mediated responses in imiquimod-induced psoriasis-like skin lesions. *J Investig Dermatol* 2013; 133(2):479-88.
33. Harb H, Stephen-Victor E, Crestani E, *et al*. A regulatory T cell Notch4-GDF15 axis licenses tissue inflammation in asthma. *Nat Immunol* 2020; 21(11):1359-70.
34. Shrestha Palikhe N, Wu Y, Konrad E, Gandhi VD, Rowe BH, Vliagoftis H. Th2 cell markers in peripheral blood increase during an acute asthma exacerbation. *Allergy* 2021; 76(1):281-90.
35. Koch S, Sopel N, Finotto S. Th9 and other IL-9-producing cells in allergic asthma. *Semin Immunopathol* 2017; 39(1):55-68.
36. Zhu M, Liang Z, Wang T, Chen R, Wang G, Ji Y. Th1/Th2/Th17 cells imbalance in patients with asthma with and without psychological symptoms. *Allergy Asthma Proc* 2016; 37(2):148-56.
37. Vyas SP, Hansda AK, Kaplan MH. Calcitriol regulates the differentiation of IL-9-secreting Th9 cells by modulating the transcription factor PU.1. *J Immunol* 2020; 204(5):1201-13.
38. Tong R, Xu L, Liang L, Huang H, Wang R, Zhang Y. Analysis of the levels of Th9 cells and cytokines in the peripheral blood of mice with bronchial asthma. *Exp Ther Med* 2018; 15(3):2480-4.
39. Saeki M, Kaminuma O, Nishimura T, Kitamura N, Mori A, Hiroi T. Th9 cells elicit eosinophil-independent bronchial hyperresponsiveness in mice. *Allergol Int* 2016; 65 : S24-9.
40. Wu X, Jiang W, Wang X, Zhang C, Cai J, Yu S, *et al*. SGK1 enhances Th9 cell differentiation and airway inflammation through NF-κB signaling pathway in asthma. *Cell Tissue Res* 2020; 382(3):563-74.
41. Newcomb DC, , Peebles Jr RS. . Th17-mediated inflammation in asthma. *Curr Opin Immunol* 2013; 25(6):755-60.
42. Zhang C, Song Y, Wang C, *et al*. The effects of chrysophanol on ovalbumin (OVA)-induced chronic lung toxicology by inhibiting Th17 response. *Toxicol Mech Methods* 2017; 27(5):327-34.
43. Irvin C, Zafar I, Good J, *et al*. Increased frequency of dual-positive TH2/TH17 cells in bronchoalveolar lavage fluid characterizes a population of patients with severe asthma. *J Allergy Clin Immunol* 2014; 134(5):Error: FPage (1175) is higher than LPage (86e7)!.
44. Mueller SN, Gebhardt T, Carbone FR, Heath WR. Memory T cell subsets, migration patterns, and tissue residence. *Annu Rev Immunol* 2013; 31 : 137-61.
45. Sallusto F, Geginat J, Lanzavecchia A. Central memory and effector memory T cell subsets: function, generation and maintenance. *Annu Rev Immunol* 2004; 22 : 745-63.
46. Gao P, Tang K, Lu Y, *et al*. Pentraxin 3 promotes airway inflammation in experimental asthma. *Respir Res* 2020; 21(1):237.
47. Kaczmarek KA, Clifford RL, Knox AJ. Epigenetic changes in airway smooth muscle as a driver of airway inflammation and remodeling in asthma. *Chest* 2019; 155(4):816-24.
48. Cheng Q, Shang Y. ORMDL3 may participate in the pathogenesis of bronchial epithelial-mesenchymal transition in asthmatic mice with airway remodeling. *Mol Med Rep* 2018; 17 (1):995-1005.
49. Liu T, Liu Y, Miller M, *et al*. Autophagy plays a role in FSTL1-induced epithelial mesenchymal transition and airway remodeling in asthma. *Am J Physiol Lung Cell Mol Physiol* 2017; 313(1):L27-40.
50. Feng H, Liu Q, Zhang N, *et al*. Leptin promotes metastasis by inducing an epithelial-mesenchymal transition in A549 lung cancer cells. *Oncol Res* 2013; 21(3):165-71.
51. Yuan J, Chen L, Xiao J, *et al*. SHROOM2 inhibits tumor metastasis through RhoA-ROCK pathway-dependent and -independent mechanisms in nasopharyngeal carcinoma. *Cell Death Dis* 2019; 10(2):58.
52. Sohal SS, Ward C, Walters EH. Importance of epithelial mesenchymal transition (EMT) in COPD and asthma. *Thorax* 2014; 69(8):768.
53. Michalik M, Wójcik-Pszczoła K, Paw M, *et al*. Fibroblast-to-myofibroblast transition in bronchial asthma. *Cell Mol Life Sci* 2018; 75(21):3943-61.
54. Tan M, Liu C, Huang W, Deng L, Qin X, Xiang Y. CTNNAL1 inhibits ozone-induced epithelial-mesenchymal transition in human bronchial epithelial cells. *Exp Physiol* 2018; 103(8): 1157-69.
55. Zhu X, Li Q, Hu G, *et al*. BMS-345541 inhibits airway inflammation and epithelial-mesenchymal transition in airway remodeling of asthmatic mice. *Int J Mol Med* 2018; 42(4):1998-2008.
56. Doerner AM, Zuraw BL. TGF-beta1 induced epithelial to mesenchymal transition (EMT) in human bronchial epithelial cells is enhanced by IL-1beta but not abrogated by corticosteroids. *Respir Res* 2009; 10(1):100.
57. Zong W, Yu C, Wang P, Dong L. Overexpression of SASH1 inhibits TGF-β1-induced EMT in gastric cancer cells. *Oncol Res* 2016; 24(1):17-23.
58. Liu F, Shang YX. Sirtuin 6 attenuates epithelial-mesenchymal transition by suppressing the TGF-β1/Smad3 pathway and c-Jun in asthma models. *Int Immunopharmacol* 2020; 82 : 106333.
59. Huang ZX, Mao XM, Wu RF, *et al*. RhoA/ROCK pathway mediates the effect of oestrogen on regulating epithelial-mesenchymal transition and proliferation in endometriosis. *J Cell Mol Med* 2020; 24(18):10693-704.
60. Xu C, Wu X, Lu M, *et al*. Protein tyrosine phosphatase 11 acts through RhoA/ROCK to regulate eosinophil accumulation in the allergic airway. *FASEB J* 2019; 33 (11):11706-20.
61. Dong Z, Tai W, Lei W, Wang Y, Li Z, Zhang T. IL-27 inhibits the TGF-β1-induced epithelial-mesenchymal transition in alveolar epithelial cells. *BMC Cell Biol* 2016; 17 : 7.
62. Ge H, Yin N, Han TL, *et al*. Interleukin-27 inhibits trophoblast cell invasion and migration by affecting the epithelial-mesenchymal transition in preeclampsia. *Reprod Sci* 2019; 26(7):928-38.